

2.20 On the Development of a Deterministic Three-Dimensional Radiation Transport Code

On the Development of a Deterministic Three-Dimensional Radiation Transport Code

Candice Rockell & John Tweed
Old Dominion University
crockell@odu.edu jtweed@odu.edu

Abstract. Since astronauts on future deep space missions will be exposed to dangerous radiations, there is a need to accurately model the transport of radiation through shielding materials and to estimate the received radiation dose. In response to this need a three dimensional deterministic code for space radiation transport is now under development. The new code, GRNTRN, is based on a Green's function solution of the Boltzmann transport equation that is constructed in the form of a Neumann series. Analytical approximations will be obtained for the first three terms of the Neumann series and the remainder will be estimated by a non-perturbative technique. This work discusses progress made to date and exhibits some computations based on the first two Neumann series terms.

1.0 INTRODUCTION

A recent National Research Council Report on the management of space radiation risk [1] highlights the need for an accurate and efficient three dimensional radiation transport code to determine and verify shielding requirements. According to this report, predictions derived from radiation transport calculations need to be tested using a common code for laboratory and space measurements that have been validated with accelerator results. Studies by Wilson et al. [2,3] have identified Green's function techniques as the likely means of generating efficient high charge and energy (HZE) shielding codes that are suitable for space engineering and are capable of being validated in laboratory experiments. In consequence, a laboratory code designed to simulate the transport of heavy ions through one or more layers of material was developed at NASA Langley Research Center [2,4,5,6,7]. It was based on a Green's function model as a perturbation series with non-perturbative corrections. This early code used a scale factor to equate range-energy relations of one material thickness into an equivalent amount of another material, and proceeded to perform the transport calculations in the new material [8]. This method proved to be acceptable for use with low-resolution detectors [6,9], but is unsuited for high-resolution measurements. Range and energy straggling, multiple Coulomb

scattering and energy downshift and dispersion associated with nuclear events were also lacking from the prior solutions. In recent publications [10,11], it has been shown how these effects can be incorporated into the multiple fragmentation perturbation series leading to the development of a new Green's function code GRNTRN (a GReeN's function code for ion beam TRaNsport). GRNTRN has accurately modeled the transport of ion beams through multilayer materials [9,12,13] and unlike earlier codes it does not make use of range scaling. It is, however, deficient in that no account is taken of the variation of particle flux with angle since the code is purely one dimensional. The present paper strives to remove this deficiency by using generalizations of previous work to develop a fully three dimensional GRNTRN code and reports on progress made towards that end.

2.0 BODY

Consideration is given to the transport of high charge and energy ions through a three-dimensional convex region V , that is bounded by a smooth surface ∂V , and is filled with a target material. It is assumed that ∂V is subject to a boundary condition of the form

$$\phi_j(\mathbf{x}_b, \boldsymbol{\Omega}, E) = F_j(\mathbf{x}_b, \boldsymbol{\Omega}, E), \quad (1)$$

where $F_j(\mathbf{x}_b, \mathbf{\Omega}, E)$ is a prescribed function, and \mathbf{x}_b is a point on the boundary. It is required that $\mathbf{\Omega} \cdot \mathbf{n}(x_b) < 0$, where $\mathbf{n}(x_b)$ is the unit outward normal at $\mathbf{x}_b \in \partial V$, and the index j takes on values from 1 to N , where N is the number of ions in the model. $\phi_j(\mathbf{x}, \mathbf{\Omega}, E)$ is the flux of j -type ions with atomic mass A_j , at $\mathbf{x} \in V$, moving in the direction $\mathbf{\Omega}$ with energy E in units of MeV/amu.

2.1 Transport Theory

According to Wilson [14], the flux is given by the transport integral equation

$$\begin{aligned} \phi_j(\mathbf{x}, \mathbf{\Omega}, E) &= \frac{P_j(\bar{E}_j) \tilde{S}_j(\bar{E}_j)}{P_j(E) \tilde{S}_j(E)} F_j[\mathbf{x}'(\mathbf{x}, \mathbf{\Omega}), \mathbf{\Omega}, \bar{E}_j] \\ &+ \sum_{k>j}^N \int_{\rho'}^{\rho} \frac{P_j(E'') \tilde{S}_j(E'') d\rho''}{P_j(E) \tilde{S}_j(E)} \int_{E''}^{\infty} dE' \int_{4\pi} d\Omega' \\ &\cdot \sigma_{jk}(\mathbf{\Omega}, \mathbf{\Omega}', E'', E') \phi_k(\mathbf{x}_n + \rho'' \mathbf{\Omega}, \mathbf{\Omega}', E'), \quad (2) \end{aligned}$$

where $\rho = \mathbf{x} \cdot \mathbf{\Omega}$, $\mathbf{x}' = \mathbf{x} - (\rho - \rho') \mathbf{\Omega}$ is the point where the ray through \mathbf{x} in the direction $\mathbf{\Omega}$ enters V , $\tilde{S}_j(E)$ is the stopping power, $P_j(E)$ is the nuclear attenuation function and $\sigma_{jk}(\mathbf{\Omega}, \mathbf{\Omega}', E, E')$ is the production cross section for j -type ions with energy E and direction $\mathbf{\Omega}$ by the collision of k -type ions with energy E' and direction $\mathbf{\Omega}'$. In addition \bar{E}_j and E'' are defined by $\bar{E}_j = \bar{E}_j(\rho - \rho', E) \equiv R_j^{-1}[R_j(E) + \rho - \rho']$, and $E'' = \bar{E}_j(\rho - \rho', E)$ where $R_j(E)$ is the usual range-energy relation.

The production cross sections used in this paper are based on S. R. Blattnig's model, which is fully described in reference [17]. They are given by the approximation

$$\begin{aligned} &\sigma_{jk}(\mathbf{\Omega}, \mathbf{\Omega}_k, E, E_k) \\ &\approx \sigma_{jk}(E_k) f_E(E, E_k) f_{\Omega}(\mathbf{\Omega}, \mathbf{\Omega}_k, E_k), \quad (3) \end{aligned}$$

where

$$f_E(E, E_k) = \frac{\exp\left(-\frac{(E_k - E_s - E)^2}{2\sigma^2 \gamma_L^2 \beta_L^2}\right)}{(2\pi)^{\frac{1}{2}} \sigma \gamma_L \beta_L}, \quad (4)$$

$$\begin{aligned} f_{\Omega}(\mathbf{\Omega}, \mathbf{\Omega}_k, E_k) &= H[\pi/2 - \theta] \frac{\gamma_L^2 \beta_L^2 m_p^2 \cos \theta}{2\pi \sigma^2} \\ &\cdot \exp\left(-\frac{\gamma_L^2 \beta_L^2 m_p^2 \sin^2 \theta}{2\sigma^2}\right). \quad (5) \end{aligned}$$

and $\sigma_{jk}(E_k)$ is the total cross section. In these equations, m_p is the proton rest mass, γ_L and β_L are parameters associated with the Lorentz transformation from the fragment reference frame to the lab frame, $\theta = \cos^{-1}(\mathbf{\Omega} \cdot \mathbf{\Omega}_k)$ is the lab frame scattering angle, E_s is the lab frame energy shift, and σ the corresponding fragment momentum width [15, 16].

By introducing the field vector

$$\Phi(\mathbf{x}, \mathbf{\Omega}, E) = [\phi_j(\mathbf{x}, \mathbf{\Omega}, E)], \quad (6)$$

the fragmentation operator Ξ

$$\begin{aligned} [\Xi \cdot \Phi]_j(\mathbf{x}, \mathbf{\Omega}, E) &= \sum_{k>j}^N \int_E^{\infty} dE' \int_{4\pi} d\Omega' \\ &\cdot \sigma_{jk}(\mathbf{\Omega}, \mathbf{\Omega}', E, E') \phi_k(\mathbf{x}, \mathbf{\Omega}', E'), \quad (7) \end{aligned}$$

and the linear transport operator \mathbf{L}

$$\begin{aligned} [\mathbf{L} \cdot \mathbf{f}(\mathbf{\Omega}_1, E_1)]_j(\mathbf{x}, \mathbf{x}'', \mathbf{\Omega}, E) \\ = \frac{P_j(E'') \tilde{S}_j(E'')}{P_j(E) \tilde{S}_j(E)} f_j(\mathbf{\Omega}, E''), \quad (8) \end{aligned}$$

the transport integral equation can be expressed in the operator form

$$\Phi = \mathbf{G}^0 \cdot \mathbf{F} + \mathbf{Q} \cdot \mathbf{L} \cdot \Xi \cdot \Phi \quad (9)$$

where \mathbf{Q} represents the integral with respect to ρ'' . Since Eq. (9) is a Volterra

type integral equation, it admits the Neumann series solution [10]

$$\Phi = \sum_{n=0}^{\infty} (\mathbf{Q} \cdot \mathbf{L} \cdot \Xi)^n \cdot \mathbf{G}^0 \cdot \mathbf{F} = \sum_{n=0}^{\infty} \mathbf{G}^n \cdot \mathbf{F} \quad (10)$$

where \mathbf{F} is the boundary flux vector and for $n \geq 1$,

$$\mathbf{G}^n = (\mathbf{Q} \cdot \mathbf{L} \cdot \Xi) \cdot \mathbf{G}^{n-1}. \quad (11)$$

In this solution, the term $\mathbf{G}^0 \cdot \mathbf{F}$ represents the primary flux vector and the term $\mathbf{G}^n \cdot \mathbf{F}$ represents the flux of the n^{th} generation of secondary ions produced.

When the boundary condition (1) takes the special form

$$\phi_j(\mathbf{x}_b, \mathbf{\Omega}, E) = \frac{\delta_{jm}}{2\pi} \delta(1 - \mathbf{\Omega} \cdot \mathbf{\Omega}_0) \cdot \delta(E - E_0) \bar{\delta}(\mathbf{x}_b - \mathbf{x}_0) \quad (12)$$

where $\bar{\delta}$ is the 'surface delta function' on ∂V , the solution of Eq. (2) is called the Green's function and is denoted by the symbol $G_{jm}(\mathbf{x}, \mathbf{x}_0, \mathbf{\Omega}, \mathbf{\Omega}_0, E, E_0)$. Once the Green's function is known, the solution for an arbitrary boundary condition (1) can be obtained from the formula

$$\begin{aligned} \phi_j(\mathbf{x}, \mathbf{\Omega}, E) &= [\mathbf{G} \cdot \mathbf{F}]_j(\mathbf{x}, \mathbf{\Omega}, E) \\ &= \sum_{k \geq j} \int_{\partial V} d\mathbf{x}_0 \int_{4\pi} d\Omega_0 \int_E^{\infty} dE_0 \\ &\cdot G_{jk}(\mathbf{x}, \mathbf{x}_0, \mathbf{\Omega}, \mathbf{\Omega}_0, E, E_0) F_k(\mathbf{x}_0, \mathbf{\Omega}_0, E_0). \quad (13) \end{aligned}$$

The summation is taken over $k \geq j$ (instead of $k > j$) to account for the primary ion spectrum.

2.2 The Zero Order Green's Function

The zero order Green's function is the first term in the Neumann series (10) with the unit boundary condition (12). On taking account of energy straggling, as described

in [10] and [11], it can be shown that the zero order Green's function takes the form

$$\begin{aligned} G_{jm}^0(\mathbf{x}, \mathbf{x}_0, \mathbf{\Omega}, \mathbf{\Omega}_0, E, E_0) &= \frac{P_m(\bar{E}_m) \delta_{jm} \delta(1 - \mathbf{\Omega} \cdot \mathbf{\Omega}_0) \bar{\delta}(\mathbf{x}' - \mathbf{x}_0)}{P_m(E) 2\pi \sqrt{2\pi} s_m(\rho - \rho', E_0)} \\ &\cdot \exp\left\{ -\frac{[E - \hat{E}_m(\rho - \rho', E_0)]^2}{2s_m(\rho - \rho', E_0)^2} \right\} \quad (14) \end{aligned}$$

where $\bar{E}_m = \bar{E}_m(\rho - \rho', E)$ and, by definition, $\hat{E}_m = \hat{E}_m(\rho - \rho', E_0) \equiv R_m^{-1}[R_m(E_0) - (\rho - \rho')]$ is the mean energy at depth $(\rho - \rho')$ g/cm² of an m-type ion that entered the transport material with energy E_0 MeV/amu, and $s_m(\rho - \rho', E_0)$ is the corresponding energy straggling width.

When the boundary condition takes the more general form (1), the primary flux is given by

$$\begin{aligned} \phi_j^0(\mathbf{x}, \mathbf{\Omega}, E) &= [\mathbf{G}^0 \cdot \mathbf{F}]_j(\mathbf{x}, \mathbf{\Omega}, E) \\ &= \int_{\partial V} d\mathbf{x}_0 \int_{4\pi} d\Omega_0 \int_E^{\infty} dE_0 \\ &\cdot G_{jj}^0(\mathbf{x}, \mathbf{x}_0, \mathbf{\Omega}, \mathbf{\Omega}_0, E, E_0) F_j(\mathbf{x}_0, \mathbf{\Omega}_0, E_0), \quad (15) \end{aligned}$$

which, in general, needs to be evaluated numerically. In the accelerator beam model described below however, Eq. (15) can be approximated analytically and a closed form expression obtained for the zero order primary flux. The result obtained in this case is called the broad zero order Green's function.

Since ion beam experiments play an important role in analyzing the shielding requirements against dangerous space radiations, there is interest in modeling the propagation of linear accelerator beams through potential shielding materials. A simple model can be constructed by assuming that the accelerator beam consists of m-type ions with mean energy E_0 MeV/amu and mean direction $\mathbf{\Omega}_0$. It is further assumed that the beam has

Gaussian profiles in both angle and energy and that it enters the material at points that are distributed in a Gaussian manner about the mean point of entry \mathbf{x}_0 . In order to accomplish this, it is assumed that the boundary ∂V is defined by the single-valued, continuously differentiable parametric equations

$$\partial V = \{\mathbf{x} : \mathbf{x} = \mathbf{x}(u, v), u_s \leq u \leq u_f, v_s \leq v \leq v_f\},$$

in which case the element of surface area is given by $dS = |\partial_u \mathbf{x} \times \partial_v \mathbf{x}| du dv$ and the surface delta function is given by

$$\bar{\delta}(\mathbf{x} - \mathbf{x}_0) = |\partial_u \mathbf{x}_0 \times \partial_v \mathbf{x}_0|^{-1} \delta(u - u_0) \delta(v - v_0).$$

The boundary condition (1) may then be assumed to take the Gaussian form

$$F_j(\mathbf{x}_b, \mathbf{\Omega}, E) = \frac{\delta_{jm}}{4\pi s_x^2 s_\Omega s_E K_x K_\Omega |\partial_u \mathbf{x}_b \times \partial_v \mathbf{x}_b|} \cdot \exp\left\{-\frac{(u_b - u_0)^2 + (v_b - v_0)^2}{2s_x^2}\right\} \exp\left\{-\frac{(E - E_0)^2}{2s_E^2}\right\} \cdot \exp\left\{-\frac{(1 - \mathbf{\Omega} \cdot \mathbf{\Omega}_0)^2}{2s_\Omega^2}\right\}, \quad (16)$$

where $\mathbf{x}_b = x_b(u_b, v_b)$, s_x, s_Ω and s_E are the spreads in space, angle and energy respectively, and K_Ω, K_x are normalization constants. It should be observed that in the limit as $s_x, s_\Omega, s_E \rightarrow 0$, the boundary condition (16) reduces to the Green's function boundary condition (12).

Equation (16) may now be substituted into Eq. (15) and the resulting integrals approximated by the mean value theorem and saddle point techniques discussed in [10]. The primary flux, which in this case is called the broad zero order Green's function $G_{jm}^b(\mathbf{x}, \mathbf{x}_0, \mathbf{\Omega}, \mathbf{\Omega}_0, E, E_0)$, is then given by the expression

$$G_{jm}^b(\mathbf{x}, \mathbf{x}_0, \mathbf{\Omega}, \mathbf{\Omega}_0, E, E_0) \approx \frac{P_m(\bar{E}_m)}{P_m(E)} \frac{\delta_{jm} H[-\mathbf{\Omega} \cdot \mathbf{n}(\mathbf{x}')] }{4\pi K_x K_\Omega |\partial_u \mathbf{x} \times \partial_v \mathbf{x}| s_x^2 s_\Omega s_m^b (\rho - \rho', E_0)} \cdot \exp\left\{-\frac{(u' - u_0)^2 + (v' - v_0)^2}{2s_x^2}\right\} \cdot \exp\left\{-\frac{(1 - \mathbf{\Omega} \cdot \mathbf{\Omega}_0)^2}{2s_\Omega^2}\right\} \cdot \exp\left\{-\frac{[E - \hat{E}_m(\rho - \rho', E_0)]^2}{2s_m^b (\rho - \rho', E_0)^2}\right\} \quad (17)$$

where

$$s_m^b (\rho - \rho', E_0)^2 = s_m (\rho - \rho', E_0)^2 + \left(\frac{\tilde{S}_m[\hat{E}_m(\rho - \rho', E_0)]}{\tilde{S}_m[E_0]}\right)^2 s_E^2. \quad (18)$$

2.3 The First Order Green's Function

The first order Green's function is given by the second term of the Neumann series (10) with the unit boundary condition (12). Since boundary condition (12) is a special case of the boundary condition (16), only the latter will be discussed. It may be recalled that the first generation fragment flux is determined by the formula

$\mathbf{G}^1 = (\mathbf{Q} \cdot \mathbf{L} \cdot \mathbf{\Xi}) \cdot \mathbf{G}^0$. Therefore, on replacing \mathbf{G}^0 by the broad zero order Green's function \mathbf{G}^b and expanding the result, it is found that the broad first order Green's function is given by the expression

$$G_{jm}^1(\mathbf{x}, \mathbf{x}_0, \mathbf{\Omega}, \mathbf{\Omega}_0, E, E_0) = \int_{\rho'}^{\rho} d\rho'' \frac{P_j(E'') \tilde{S}_j(E'')}{P_j(E) \tilde{S}_j(E)} \int_{E''}^{\infty} dE_1 \int_{4\pi} d\Omega_1 \frac{H[-\mathbf{\Omega}_1 \cdot \mathbf{n}(\mathbf{x}_1')] \sigma_{jm}(\mathbf{\Omega}, \mathbf{\Omega}_1, E'', E_1)}{|\partial_u \mathbf{x}_1 \times \partial_v \mathbf{x}_1| s_x^2 s_\Omega s_m^b (\rho_1'' - \rho_1', E_0)}$$

$$\frac{P_m[\bar{E}_m(\rho_1'' - \rho_1', E_1)]}{4\pi K_x K_\Omega P_m[E_1]} \exp\left\{-\frac{(u_1' - u_0)^2 + (v_1' - v_0)^2}{2s_x^2}\right\} \cdot \exp\left\{-\frac{[E_1 - \hat{E}_m(\rho_1'' - \rho_1', E_0)]^2}{2s_m^b(\rho_1'' - \rho_1', E_0)^2}\right\} \cdot \exp\left\{-\frac{(1 - \Omega_1 \cdot \Omega_0)^2}{2s_\Omega^2}\right\}, \quad (19)$$

$$\frac{C'_{jm}(\rho^*)s_m^1(\rho^*)}{\sqrt{2\pi}g'_{jm}(\rho^*)^2} \cdot \left\{ \exp\left(\frac{-g_{jm}(\rho)^2}{2s_m^1(\rho^*)^2}\right) - \exp\left(\frac{-g_{jm}(\rho')^2}{2s_m^1(\rho^*)^2}\right) \right\}, \quad (21)$$

ρ^* is the root of the equation $g_{jm}(\rho'') = 0$,

$$g_{jm}(\rho'') = \hat{E}_m(\rho'' - \rho, E_0) - E_s[\hat{E}_m(\rho'' - \rho, E_0)] - \bar{E}_j(\rho - \rho'', E), \quad (22)$$

$$s_m^1(\rho^*)^2 = s_m^b(\rho^* - \rho', E_0)^2 + \sigma^2 \gamma_L [\hat{E}_m(\rho - \rho^*, E_0)]^2 \beta_L [\hat{E}_m(\rho - \rho^*, E_0)]^2, \quad (23)$$

and

$$C_{jm}(\rho'') = \frac{\tilde{S}_j[\bar{E}_j(\rho - \rho'', E)]P_m(E_0)}{\tilde{S}_j(E)P_j(E)} \cdot \frac{P_j[\bar{E}_j(\rho - \rho'', E)]}{P_m[\hat{E}_m(\rho - \rho'', E_0)]} \sigma_{jm}[\hat{E}_m(\rho - \rho'', E_0)]. \quad (24)$$

where $\rho_1'' = \mathbf{x}'' \cdot \Omega_1$, $\mathbf{x}_1' = \mathbf{x}'' - (\rho_1'' - \rho_1')\Omega_1$ is the point where the ray through \mathbf{x}'' , in the direction Ω_1 enters V , $\bar{E}_m = \bar{E}_m(\rho_1'' - \rho_1', E_1)$, $\hat{E}_m = \hat{E}_m(\rho_1'' - \rho_1', E_0)$ is the mean energy at depth $(\rho_1'' - \rho_1')$ g/cm² of an m-type ion that entered the transport material with energy E_0 MeV/amu, and $s_m^b(\rho_1'' - \rho_1', E_0)$ is the corresponding energy width.

The expression in Eq. (19) can be evaluated by numerical quadrature, but this is computationally expensive and therefore it is desirable to construct an analytical approximation. This can be done by making use of Taylor's theorem, the mean value theorem, and saddle point techniques as described in [10], and yields the result

$$G_{jm}^1(\mathbf{x}, \mathbf{x}_0, \Omega, \Omega_0, E, E_0) = \frac{H[-\Omega \cdot \mathbf{n}(\mathbf{x}')] }{(2\pi)^{\frac{3}{2}} K_x K_\Omega s_x^2 s_\Omega} \cdot \frac{1}{|\partial_u \mathbf{x} \times \partial_v \mathbf{x}'|} \exp\left\{-\frac{(u' - u_0)^2 + (v' - v_0)^2}{2s_x^2}\right\} \cdot \exp\left\{-\frac{(1 - \Omega \cdot \Omega_0)^2}{2s_\Omega^2}\right\} G_{jm}^{1b}(\rho, \rho', E, E_0), \quad (20)$$

where

$$G_{jm}^{1b}(\rho, \rho', E, E_0) = \left[\frac{C_{jm}(\rho^*)}{2g'_{jm}(\rho^*)} \right] \cdot \left\{ \operatorname{erf}\left(\frac{g_{jm}(\rho)}{\sqrt{2}s_m^1(\rho^*)}\right) - \operatorname{erf}\left(\frac{g_{jm}(\rho')}{\sqrt{2}s_m^1(\rho^*)}\right) \right\}$$

3.0 DISCUSSION

To illustrate some of the theory presented above, the case in which the boundary flux consists of the m^{th} component of the Galactic Cosmic Ray (GCR) spectrum is discussed. Since the GCR is isotropic and spatially uniform, boundary condition (1) takes the special form

$$\phi_j(\mathbf{x}_b, \Omega, E) = \delta_{jm} F_m(E), \quad (25)$$

where the spectra $F_m(E)$ are broad functions of energy. These have been modeled by Badhwar and O'Neil (1995) and made available in tabular form at a number of solar maxima and minima between the years 1958 and 1989.

In these circumstances, Eq. (15) for the primary flux takes the form

$$\begin{aligned} \phi_j^0(\mathbf{x}, \boldsymbol{\Omega}, E) &= [\mathbf{G}^0 \cdot \mathbf{F}]_j(\mathbf{x}, \boldsymbol{\Omega}, E) \\ &\approx H[-\boldsymbol{\Omega} \cdot \mathbf{n}(\mathbf{x}')] \frac{P_m(\bar{E}_m)}{P_m(E)} \int_{\mathbb{R}} \frac{\delta_{jm} F_m(E_1)}{\sqrt{2\pi s_m(\rho - \rho', E_1)}} \\ &\cdot \exp\left\{-\frac{[E - \hat{E}_m(\rho - \rho', E_1)]^2}{2s_m(\rho - \rho', E_1)^2}\right\} dE_1, \end{aligned} \quad (26)$$

and, with the help of Taylor's theorem and the mean value theorem, may be further approximated as

$$\begin{aligned} \phi_j^0(\mathbf{x}, \boldsymbol{\Omega}, E) &\approx \delta_{jm} H[-\boldsymbol{\Omega} \cdot \mathbf{n}(\mathbf{x}')] \\ &\cdot \frac{P_m(\bar{E}_m) \tilde{S}_m(\bar{E}_m)}{P_m(E) \tilde{S}_m(E)} F_m(\bar{E}_m). \end{aligned} \quad (27)$$

The first generation fragment flux also simplifies and is approximated by the expression

$$\begin{aligned} \phi_j^1(\mathbf{x}, \boldsymbol{\Omega}, E) &= [\mathbf{G}^1 \cdot \mathbf{F}]_j(\mathbf{x}, \boldsymbol{\Omega}, E) \\ &\approx H[-\boldsymbol{\Omega} \cdot \mathbf{n}(\mathbf{x}')] \\ &\cdot \int_{-\infty}^{\infty} G_{jm}^{1b}(\rho, \rho', E, E_0) F_m(E_0) dE_0 \end{aligned} \quad (28)$$

where $G_{jm}^{1b}(\rho, \rho', E, E_0)$ is the special case of $G_{jm}^{1b}(\rho, \rho', E, E_0)$ for which $s_E = 0$.

3.1 GCR on a Half-Space

In the first example to be considered, the target is an aluminum solid that occupies the half-space $V = \{(x, y, z) : z \geq 0\}$ whose boundary ∂V is the xy -plane. The Cartesian components of the vector $\boldsymbol{\Omega}$ are given by $\boldsymbol{\Omega} = (\sin \gamma \cos \alpha, \sin \gamma \sin \alpha, \cos \gamma)$ and are therefore completely determined by the polar angles γ and α . The measured GCR ^{56}Fe flux associated with the 1977 solar minimum [18] provides the boundary condition (25). The primary flux (27) then takes the form

$$\begin{aligned} \phi_j^0(\mathbf{x}, \boldsymbol{\Omega}, E) &\approx \delta_{jm} H[\cos \gamma] \\ &\cdot \frac{P_m(\bar{E}_m) \tilde{S}_m(\bar{E}_m)}{P_m(E) \tilde{S}_m(E)} F_m(\bar{E}_m), \end{aligned} \quad (29)$$

where $\bar{E}_m = \bar{E}_m(z / \cos \gamma, E)$ and $0 \leq \gamma < \pi/2$.

Since the field is axisymmetric about any line parallel to the z -axis, the fluxes of interest are functions of z, γ , and E only. Figures 1 and 2 show the variation of the ^{56}Fe primary flux with γ and E at the points (0,0,0) and (0,0,5) respectively. Figure 3 provides a similar illustration for the first generation ^{16}O fragments at the point (0,0,5).

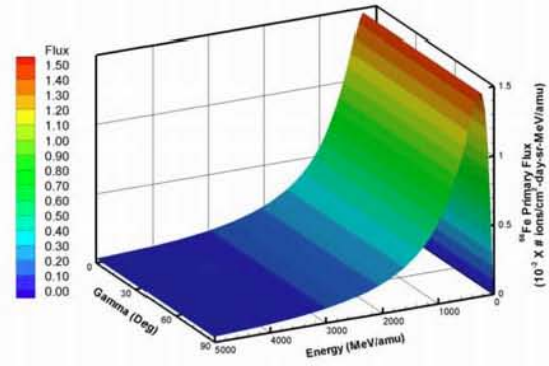


Fig 1.

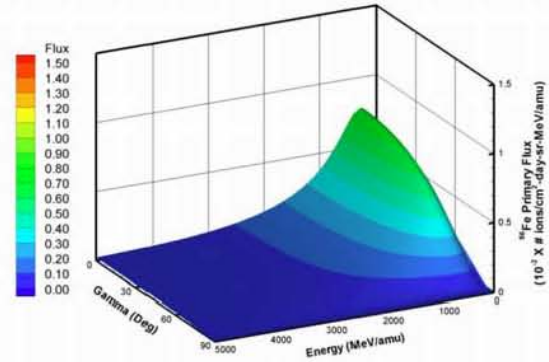


Fig 2.

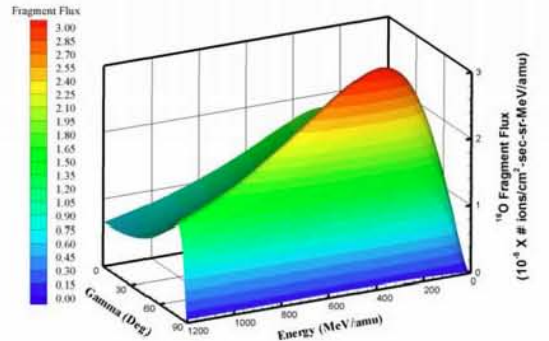


Fig 3.

3.2 GCR on a Circular Cylinder

In the second example to be considered, the target is the solid aluminum cylinder $x^2 + y^2 \leq 16^2$, $0 \leq z \leq 36$ and again the boundary condition is provided by the measured GCR ^{56}Fe flux associated with the 1977 solar minimum.

Figures 4 and 5 show the variation of the ^{56}Fe primary flux with γ and E at the points (0,0,0) and (0,0,18) respectively, where the field is axisymmetric. Similar results for the first generation ^{16}O fragment flux are shown in Figs. 6 and 7.

The remaining figures deal with the flux at the point (14,0,9) where the field is no longer axisymmetric. Figures 8 and 9 show how the ^{56}Fe primary flux varies with γ and E when $\alpha = 0^\circ$ and $\alpha = 90^\circ$ respectively. Figures 10 and 11 provide a similar illustration of the ^{16}O fragment flux.

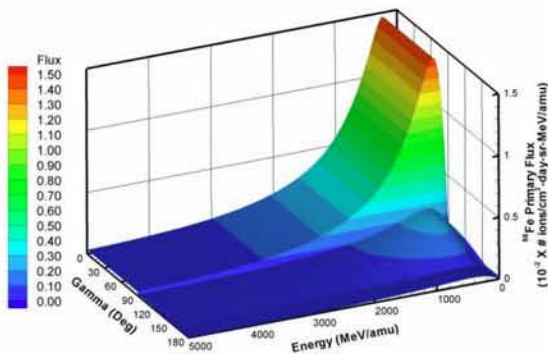


FIG 4.

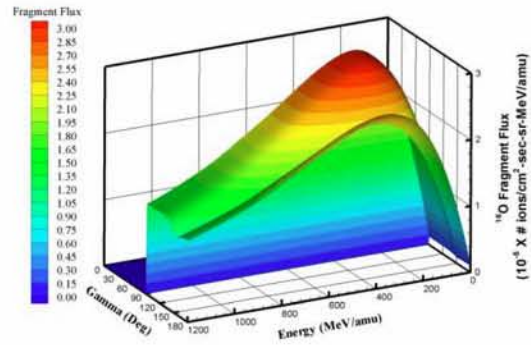


FIG 6.

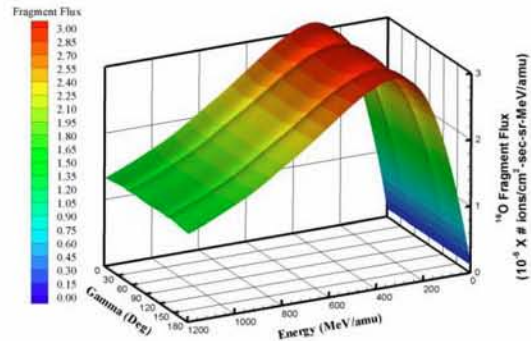


FIG 7.

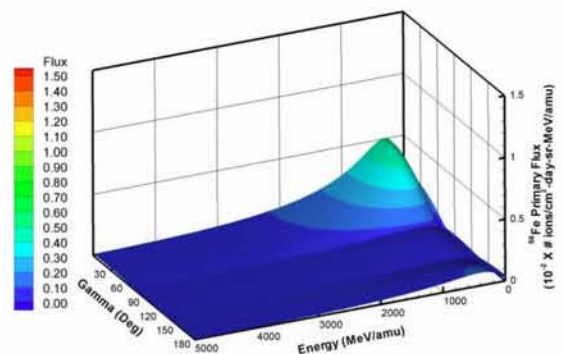


FIG 8.

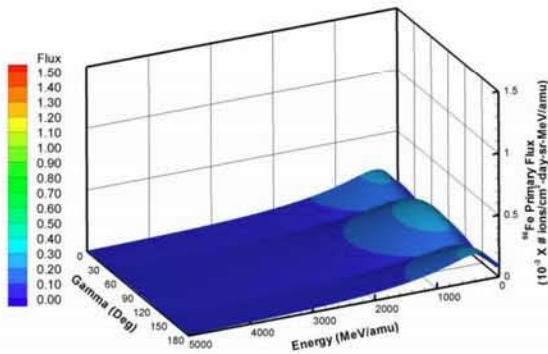


FIG 5.

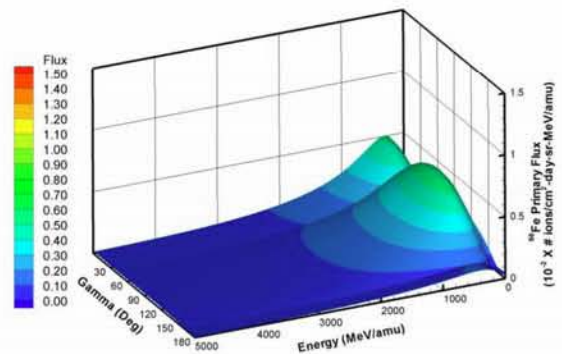


FIG 9.

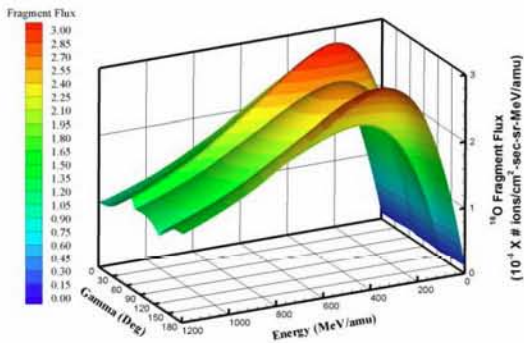


FIG 10.

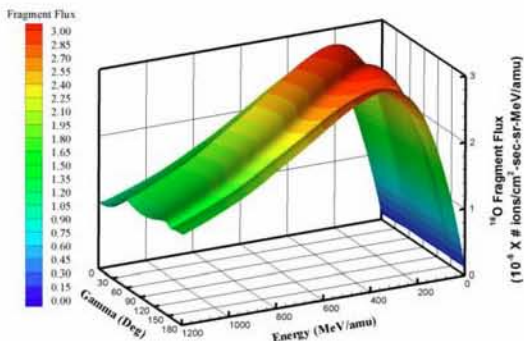


FIG 11.

4.0 CONCLUSION(S)

In this work, some progress toward the development of a fully three dimensional deterministic code for space radiation transport was discussed. Approximations were obtained for the first two terms of the Neumann series solution of the transport integral equation. The results were then illustrated by exhibiting the primary flux and the first generation ^{16}O fragment flux in a half-space, and in a circular cylinder, due to the ^{56}Fe component of the GCR.

In future work an approximation for the third Neumann series term will be obtained and the Neumann series remainder estimated by a non-perturbative technique. Predictions made by the code will then be compared with the results of laboratory beam experiments and measured space data.

5.0 REFERENCES

1. Committee on the Evaluation of Radiation Shielding for Space Exploration, *Managing Space Radiation Risk in the New Era of*

Space Exploration, The National Academies Press, Washington, D.C. (2008).

2. J. W. Wilson, L. W. Townsend, S. L. Lamkin, and B. D. Ganapol, "A closed form solution to HZE propagation," *Radiat. Res.*, **122**, 223-228 (1990).
3. J. W. Wilson, S. L. Lamkin, H. Farhat, B. D. Ganapol, and L. W. Townsend, "A hierarchy of transport approximations for high energy heavy (HZE) ions," NASA TM-4118, National Aeronautics and Space Administration (1989).
4. J. W. Wilson, F.F. Badavi, R. C. Costen and J. L. Shinn, "Non-perturbative methods in HZE transport," NASA TP-3363, National Aeronautics and Space Administration (1993).
5. J. W. Wilson, L. W. Townsend, W. Schimmerling, G. S. Khandelwal, F. Khan, J. E. Nealy, F. A. Cucinotta, L. C. Simonsen, J. L. Shinn and J. W. Norbury, "Transport Methods and Interactions for Space Radiations," NASA RP-1257, National Aeronautics and Space Administration (1991).
6. J. L. Shinn, J. W. Wilson, F.F. Badavi, E. V. Benton, I. Csige, A. L. Frank and E. R. Benton, "HZE Beam Transport in Multilayered Materials," *Radiat. Meas.*, **23**, 57-64 (1994).
7. J. L. Shinn, J. W. Wilson, W. Schimmerling, M. R. Shavers, J. Miller, E. V. Benton, A. L. Frank and F. F. Badavi, "A Green's function method for heavy ion beam transport," *Radiat. Environ. Biophys.*, **34**, 155-159 (1995).
8. J. L. Shinn, J. W. Wilson, E. V. Benton and F.F. Badavi, "Multilayer analysis of an Iron radiation beam experiment," NASA TM-4753, National Aeronautics and Space Administration (1997).
9. S. A. Walker, J. Tweed, J. W. Wilson, F. A. Cucinotta, R. K. Tripathi, S. Blattinig, C. Zeitlin, L. Heilbronn and J. Miller,, "Validation of the HZETRN code for laboratory exposures with 1 A GeV iron ions in several targets," *Adv. Space Res.*, **35**, 202-207 (2005).
10. J. Tweed, J. W. Wilson, and R. K. Tripathi, "An improved Green's function for ion beam transport," *Adv. Space Res.*, **34**, 1311-1318 (2004).
11. C. J. Mertens, S. A. Walker, J. W. Wilson, R. C. Singleterry, and J. Tweed, "Coupling of Multiple Coulomb Scattering with Energy

- Loss and Stragglings in HZETRN," *Adv. Space Res.*, 40, 1357-1367 (2007).
12. J. Tweed, S. A. Walker, J. W. Wilson, R. K. Tripathi, F. F. Badavi, J. Miller, C. Zeitlin, and L. H. Heilbronn,, "Validation Studies of the GRNTRN Code for Radiation Transport," ICES 2007-01-3118, SAE 37th International Conference on Environmental Systems, Chicago, 2007.
 13. J. Tweed, S. A. Walker, J. W. Wilson, and R. K. Tripathi, "Recent Progress in the Development of a Multi-Layer Green's Function Code for Ion Beam Transport," STAIF-2008 (Space Technology & Applications Forum), Albuquerque, NM, February 10-14, 2008. *AIP Conf. Proc.*, 969, 993-100 (2008).
 14. J. W. WILSON, "Analysis of the Theory of High-Energy Ion Transport," *NASA TN D-8381*, National Aeronautics and Space Administration (1977).
 15. L.W. Townsend, F. Khan and R. K. Tripathi, "Optical model analyses of 1.65A GeV argon fragmentation: Cross sections and momentum distributions," *Phys. Rev. C* 48, 2912-2919 (1993).
 16. R. K. Tripathi , W. Townsend and F. Khan, "Role of intrinsic width in fragment momentum distributions in heavy ion collisions," *Physical Review C*, 49, 1775-1777 (1994).
 17. C. Rockell, J. Tweed, S. R. Blattnig and C. J. Mertens, "Recent Developments in Three Dimensional Radiation transport using the Green's Function Technique," *Nuclear Science and Engineering*, (unpublished).
 18. J. W. Wilson, F.F. Badavi, F. A. Cucinotta, J. L. Shinn, G. D. Badhwar, R. Silberberg, C. H. Tsao, L. W. Townsend and R. K. Tripathi, HZETRN: Description of a Free-Space Ion and Nucleon Transport and Shielding Computer Program, NASA TP-3495, National Aeronautics and Space Administration, (1995).

6.0 ACKNOWLEDGMENTS

The author (C.R.) wishes to acknowledge the NASA support she received for this work under the Graduate Student Researchers Program (NASA NNX09AJ06H) and the Virginia Space Grant Consortium.

On the Development of a Deterministic Three-Dimensional Radiation Transport Code

Candice Rockell, John Tweed

October 13, 2010

Old Dominion University, Norfolk, VA 23529
crockell@odu.edu

1/25

Outline

Overview

- 1 *Introduction/Motivation*
- 2 *Transport Theory*
- 3 *Zero Order Green's Function*
- 4 *First Order Green's Function*
- 5 *Results*
- 6 *Conclusions and Future Work*

2/25

Radiation in Space

3 Main Types of Radiation:

- Galactic Cosmic Rays (GCR)
 - energetic charged particles
 - penetrating power
- Solar Particle Events (SPE)
 - energetic protons and alpha particles
 - not likely to fragment
- Particles Trapped in Radiation Belts

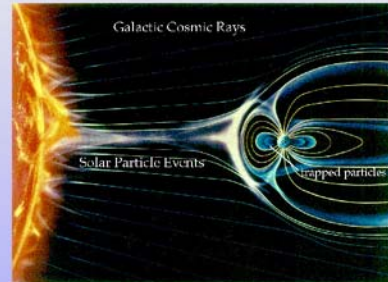


Figure: Earth's magnetosphere and its interaction with the sun.

(NASA)

3/25

Damage from Radiation

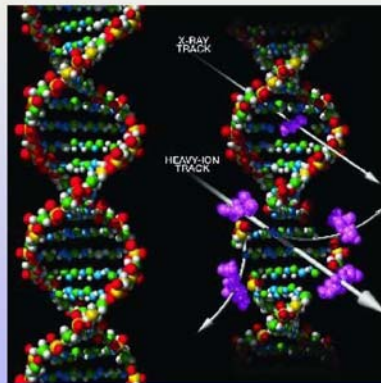


Figure: DNA Damage due to heavy ions.(NASA)

Consequently, steps must be taken to ensure astronaut safety by providing adequate shielding.

4/25

Future Space Programs

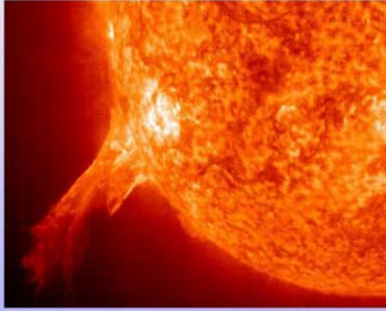
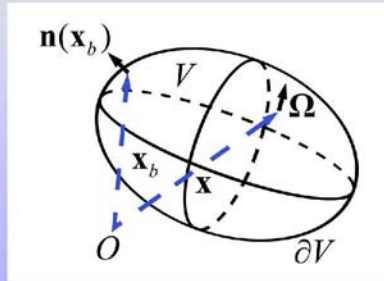


Figure: Solar Particle Events.
(NASA)

- Require accurate and efficient methods for radiation transport -
 - Determine and verify shielding requirements
- National Research Council Report -
 - Predictions need to be validated
 - Use a common code for lab and space measurements
 - Capable of being validated with accelerator results
- Green's function techniques -
 - Likely means for space engineering and lab experiments

5/25

Transport Geometry



V Convex region

∂V Boundary of V

x, x_b Position vectors of arbitrary points in V and ∂V respectively

$n(x_b)$ Unit outward normal at x_b

Ω Arbitrary unit vector at x

6/25

Volterra Integral Equation

Transport Integral Equation

$$\phi_j(\mathbf{x}, \Omega, E) = \frac{P_j(\bar{E}_j) \tilde{S}_j(\bar{E}_j)}{P_j(E) \tilde{S}_j(E)} F_j(\mathbf{x}(\mathbf{x}, \Omega), \Omega, \bar{E}_j) + \sum_{k>j} \int_{\rho'}^{\rho} \frac{P_j(E'') \tilde{S}_j(E'') d\rho''}{P_j(E) \tilde{S}_j(E)} \cdot \int_{E''}^{\infty} dE' \int_{4\pi} d\Omega' \sigma_{jk}(\Omega, \Omega', E'', E') \cdot \phi_k(\mathbf{x}_n + \rho'' \Omega, \Omega', E') \quad (1)$$

where

Ω	=	Direction of propagation
$\tilde{S}_j(E)$	=	Energy lost per unit path length per unit mass
$\sigma_j(E)$	=	Macroscopic absorption cross section
$\phi_k(\mathbf{x}, \Omega', E')$	=	Flux of k -type ions
$\sigma_{jk}(\Omega, \Omega', E, E')$	=	Double differential production cross section
$P_j(E)$	=	Nuclear survival probability

7/25

Green's Function

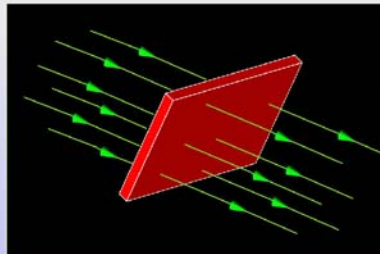


Figure: Flux of particles through a material.

The Solution: Green's Function

$$G_{jm}[\mathbf{x}, \mathbf{x}_0, \Omega, \Omega_0, E, E_0] \quad (2)$$

8/25

Neumann Series Solution

This Neumann series can be expressed as

$$\Phi = [\mathbf{G}^0 + \mathbf{G}^1 + \mathbf{G}^2 + \mathbf{G}^3 + \dots] \cdot \mathbf{F} \quad (3)$$



Figure: Atmospheric air shower. (Pierre Auger Observatory Team)

9/25

Primary Flux

The primary flux can be obtained by

$$\begin{aligned} \phi_j^0(\mathbf{x}, \Omega, E) &= [\mathbf{G}^0 \cdot \mathbf{F}]_j(\mathbf{x}, \Omega, E) \\ &= \int_{\partial V} d\mathbf{x}_0 \int_{4\pi} d\Omega_0 \int_E^\infty dE_0 \\ &\quad \cdot G_{jj}^0(\mathbf{x}, \mathbf{x}_0, \Omega, \Omega_0, E, E_0) F_j(\mathbf{x}_0, \Omega_0, E_0), \end{aligned} \quad (4)$$

which needs to be evaluated numerically for some situations.

10/25

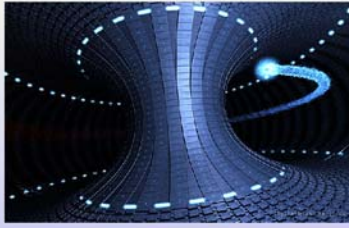
Ion Beam Experiment and the Broad Zero Order Green's Function

Figure: Ion Beam Experiment. (Ryan Bliss)

Definition

The *Broad Zero Order Green's Function* assumes that the beam has Gaussian profiles in both **angle** and **energy** and that it enters the material at points that are distributed in a Gaussian manner about the mean point of entry.

11/25

First Order Green's Function

$$\Phi = [G^0 + G^1 + G^2 + G^3 + \dots] \cdot F$$

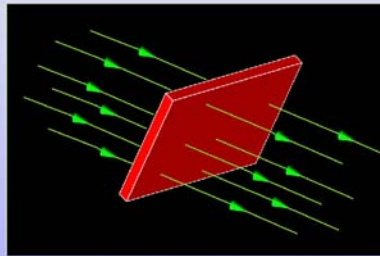


Figure: Unit Boundary Condition.

12/25

Galactic Cosmic Rays (GCR)

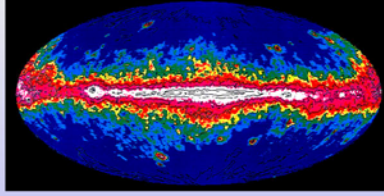


Figure: Galactic Cosmic Ray Distribution. (NASA)

$$\phi_j(\mathbf{x}_b, \Omega, E) = \delta_{jm} F_m(E)$$

where the spectra $F_m(E)$ are broad functions of energy.

13/25

GCR on a Half-Space

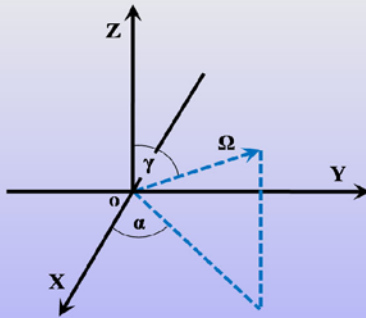


Figure: Coordinate variables.

14/25

GCR ^{56}Fe Primary flux for the 1977 solar min

$$\Phi^0 = G^0 \cdot F$$

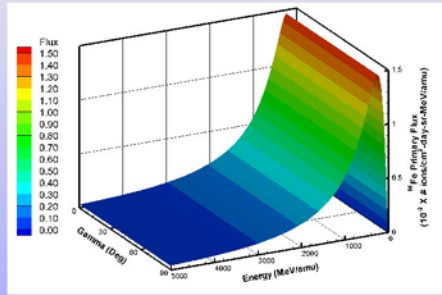


Figure: The ^{56}Fe primary ion flux at (0,0,0).

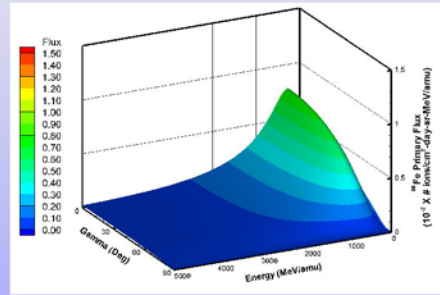


Figure: The ^{56}Fe primary ion flux at (0,0,5).

15/25

GCR ^{16}O Fragment flux for the 1977 solar min

$$\Phi^1 = G^1 \cdot F$$

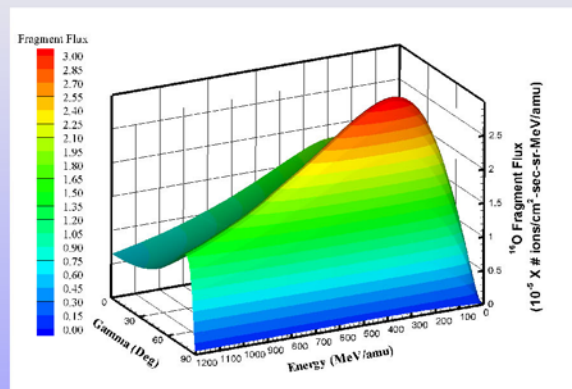


Figure: The ^{16}O fragment flux at (0,0,5).

16/25

GCR on a Circular Cylinder

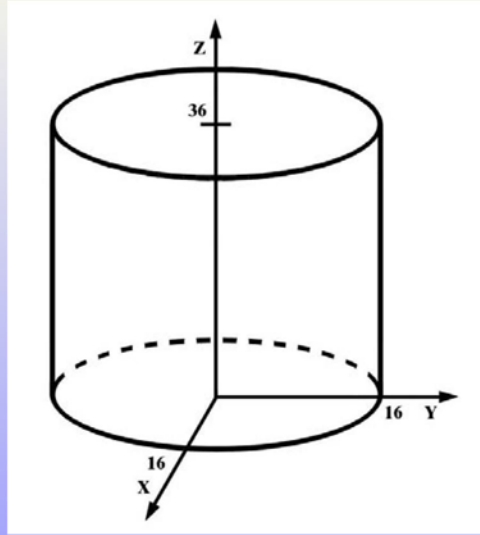


Figure: Circular Cylinder

GCR ^{56}Fe Primary flux for the 1977 solar min

$$\Phi^0 = G^0 \cdot F$$

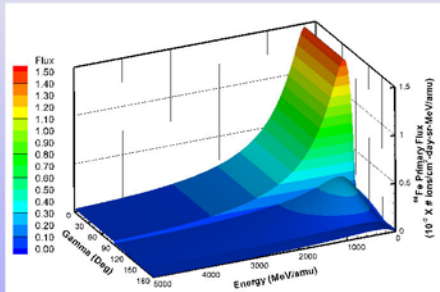


Figure: The ^{56}Fe primary ion flux at (0,0,0).

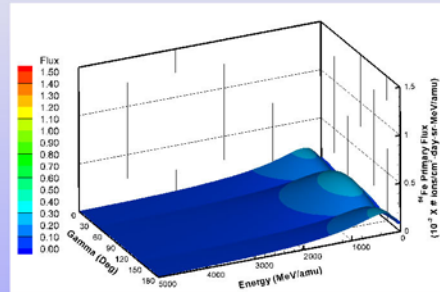


Figure: The ^{56}Fe primary ion flux at (0,0,18).

GCR ¹⁶O Fragment flux for the 1977 solar min

$$\Phi^1 = G^1 \cdot F$$

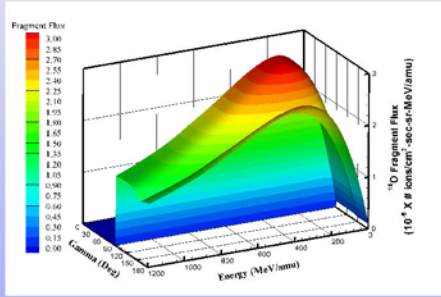


Figure: The ⁵⁶Fe primary ion flux at (0,0,0).

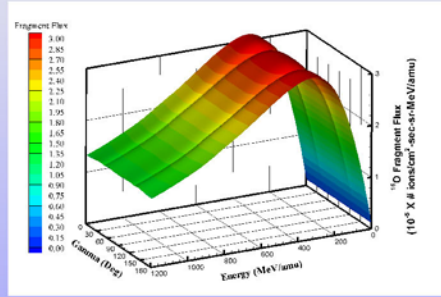


Figure: The ⁵⁶Fe primary ion flux at (0,0,18).

GCR ⁵⁶Fe Primary flux showing antisymmetry

$$\Phi^0 = G^0 \cdot F$$

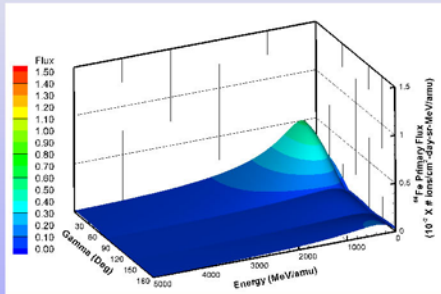


Figure: The ⁵⁶Fe primary ion flux at (14,0,9) when alpha=0 Deg.

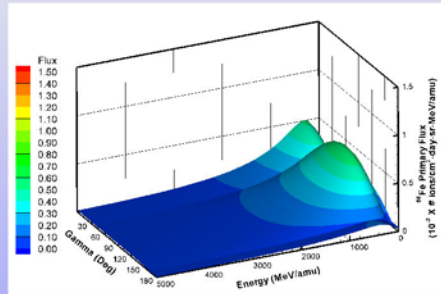


Figure: The ⁵⁶Fe primary ion flux at (14,0,9) when alpha=90 Deg.

GCR ^{16}O Fragment flux showing antisymmetry

$$\Phi^1 = G^1 \cdot F$$

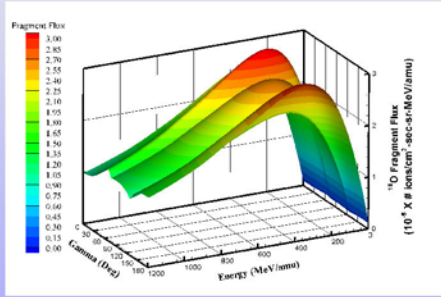


Figure: The ^{16}O fragment flux at (14,0,9) when $\alpha=0$ Deg.

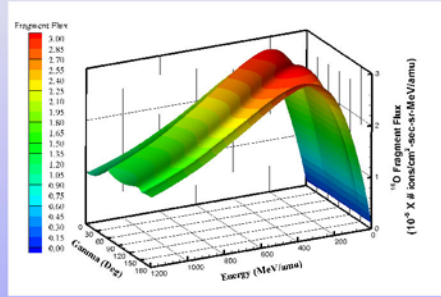


Figure: The ^{16}O fragment flux at (14,0,9) when $\alpha=90$ Deg.

Conclusions

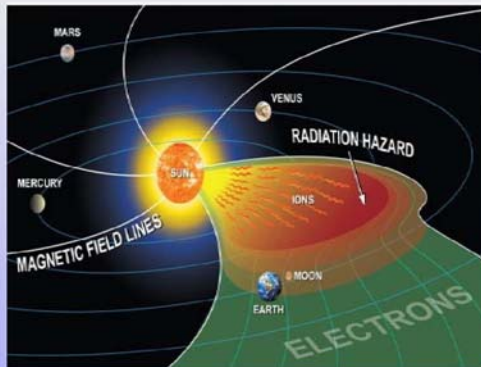


Figure: Depiction of solar radiation. (NASA)











- 1 Volterra Integral Equation
- 2 Solved using a Neumann Series solution.
 - Green's functions
 - Closed form approximations for G^0 and G^1 .
 - Showed results for the GCR boundary condition.
- 3 Future Work

Acknowledgements










I would like to acknowledge the NASA support that I received for this work under the Graduate Student Research Program (NASA NNX09AJ06H) and the Virginia Space Grant Consortium.



References

-  Committee on the Evaluation of Radiation Shielding for Space Exploration, Managing Space Radiation Risk in the New Era of Space Exploration, The National Academies Press, Washington, D.C., 2008.
-  Mertens, C., Wilson, J.W., et al., Coupling of Multiple Coulomb Scattering with Energy Loss and Straggling in HZETRN, *Advances in Space Research* 40, 1357-1367, 2007.
-  Miroshnichenko, Leonty I. *Radiation Hazard in Space*, Kluwer Academic Publishers, Boston, MA, 2003.
-  Shinn, J.L., et al, HZE Beam Transport in Multilayered Materials, *Radiation Measurements* 23, 57-64, 1994.
-  Shinn, J.L., et al, A Green's function method for heavy ion beam transport, *Radiat. Environ. Biophys* 34, 155-159, 1995.
-  Shinn, J.L., et al, Multilayer analysis of an Iron radiation beam experiment, NASA TM-4753, National Aeronautics and Space Administration, 1997.
-  Townsend, L.W., Khan, F., and Tripathi, R.K., Optical model analyses of 1.65A GeV argon fragmentation: Cross sections and momentum distributions, *Phys. Rev. C* 48, 2912-2919, 1993.
-  Tripathi, R.K., Townsend, L.W., Role of intrinsic width in fragment momentum distributions in heavy ion collisions, *Phys. Rev. C* 48, R1775-R1777, 1994.
-  Tweed, J., Wilson, J. W., Tripathi, R. K., An improved Green's function for ion beam transport, *Advances in Space Research* 34, 1311-1318, 2004.
-  Tweed, J., et al., Recent Progress in the Development of a Multi-Layer Green's Function Code for Ion Beam Transport, STAIIF-2008 (Space Technology and Applications Forum), Albuquerque, NM, February 10-14, 2008. AIP Conf. Proc. 969, 993-1000, 2008.

References

-  Tweed, J., et al, Validation Studies of the GRNTRN Code for Radiation Transport, ICES 2007-01-3118, SAE 37th International Conference on Environmental Systems, Chicago, 2007.
-  Walker, S.A, et al., Validation of the HZETRN code for laboratory exposures with 1 A GeV iron ions in several targets, Adv. Space Res. 35, 202-207, 2005.
-  Wilson, J.W., Analysis of the theory of high-energy ion transport, NASA TN D-8381, National Aeronautics and Space Administration, 1977.
-  Wilson, J.W., Badavi, F.F., Cucinotta, et al., HZETRN: Description of a Free-Space Ion and Nucleon Transport and Shielding Computer Program, NASA TP-3495, National Aeronautics and Space Administration, 1995.
-  Wilson, J. W., Townsend, L.W., Schimmerling, W., et al., Transport Methods and Interactions for Space Radiations, NASA RP-1257, National Aeronautics and Space Administration, 1991.
-  Wilson, J. W., Tweed, J., Tai, H., et al., A simple model for straggling evaluation, Nucl. Instr. and Meth. in Phys. Res. B 194, 389-392, 2002.
-  Wilson, J.W., et al, A closed form solution to HZE propagation, Radiation Research 122, 223-228, 1990.
-  Wilson, J.W., et al, A hierarchy of transport approximations for high energy heavy (HZE) ions, NASA TM-4118, National Aeronautics and Space Administration, 1989.
-  Wilson, J.W., et al, Non-perturbative methods in HZE transport, NASA TP-3363, National Aeronautics and Space Administration, 1993.